UDK 621.315.6:544.452 ISSN 1580-2949
Original scientific article/Izvirni znanstveni članek MTAEC9, 57(3)217(2023)

EXPERIMENTAL STUDY ON THE FACTORS AFFECTING THE INSULATION PERFORMANCE OF FLAME-RETARDANT MULTILAYER INSULATION MATERIALS

EKSPERIMENTALNA ŠTUDIJA DEJAVNIKOV, KI VPLIVAJO NA IZOLATIVNE LASTNOSTI VEČPLASTNIH NEGORLJIVIH IZOLACIJSKIH MATERIALOV

Xiaoyong Ma[1], Shuping Chen[1*], Lian Chen[2], Yujie Wang[2], Shufeng Jin[1], Yang Yu[3], Maoyuan Mi[1], Chaofan Shi[1], Yagang Shi[1]

[1]School of Petrochemical Engineering, Lanzhou University of Technology, Lanzhou, China
[2]Science and Technology on Vacuum Technology and Physics Laboratory, Lanzhou Institute of Physics, Lanzhou, China
[3]Institute of Refrigeration and Cryogenic Engineering, Xi'an Jiaotong University, Xi'an, China

Prejem rokopisa – received: 2023-01-05; sprejem za objavo – accepted for publication: 2023-03-07

doi:10.17222/mit.2023.736

Flame-retardant multilayer insulation materials act as effective thermal insulation blankets of cryogenic containers that store flammable and explosive cryogenic liquids. This study used standard static liquid nitrogen boil-off calorimetry to test the insulation performance of eight groups of flame-retardant multilayer insulation materials with different wrapping parameters. The effects of four factors, namely the layer density, seaming process, number of reflector layer, and variable-density multilayer insulation arrangement, on the insulation performance were analysed. Three layer densities were considered: 4.47, 3.08, and 2.50 layers/mm. Two types of seaming processes were discussed: the overlapped and fold-over seaming processes. Three numbers of reflector layers were considered: 60, 70, and 80. Two variable-density multilayer insulation arrangements with similar thicknesses were discussed: 10-10-40 and 20-20-20 layers of reflectors allocated for low-, medium- and high-density segments. The conclusions are as follows: Decreasing the layer density enhances the performance of multilayer insulation; Using the fold-over seaming process results in less heat flux and lower apparent thermal conductivity; An increase in the number of reflector layers weakens radiative heat transfer, resulting in better thermal insulation; Furthermore, for a given wrapping thickness, reducing the number of reflectors appropriately in low- and medium-density segments improves the insulation performance; Optimizing and controlling the layer density of each density segment are also essential for variable-density multilayer insulation effects. This study provides supporting theories and reference data for practical engineering applications.

Keywords: flame-retardant multilayer insulation, layer density, seaming process, variable density

Negorljivi večplastni izolacijski materiali oz. materiali, ki vsebujejo zaviralce gorenja delujejo kot učinkovite toplotno izolativne blazine oz. obloge kriogenih zabojnikih v katerih so shranjene gorljive in/ali eksplozivne kriogene kapljevine.V študiji so avtorji uporabili standardno statično kalorimetrijo s tekočim dušikom za ugotavljanje izolativnih lastnosti osmih skupin večplastnih izolativnih negorljivih materialov z različnimi parametri zaviranja gorenja. Analizirali in ugotavljali so učinke štirih parametrov: gostote plasti, procesa šivanja oz. robljenja, števila plasti oz.števila odbojnih plasti ter razporeditve posameznih plasti. Ocenjevali so vpliv treh različnih gostot:4,47, 3,08 in 2,50 plasti/mm. Obravnavali oz. izbrali so dva tipa procesovšivanja oz. robljenja: s prekrivanjem in z zgibanjem. Ocenjevali so tri različna števila odbojnih oz. zaviralnih plasti: 60, 70 in 80. Obravnavali so dve različni razporeditvi izolacijskih plasti s podobno gostoto in sicer 10-10-40 ter 20-20-20 odbojnih plasti v delih z nizko, srednjo in visoko gostoto. Na osnovi rezultatov analiz so ugotavili, da zmanjševanje gostote plasti izboljšuje izolativne lastnosti izbranih večplastnih materialov. Uporaba procesa šivanja oz. robljenja večplastnih materialov s postopkom zgibanja zmanjšuje toplotni tok in znižuje navidezno toplotno prevodnost materialov. Povečanje števila odbojnih plastislabi prenos toplote s sevanjem, kar se odraža v boljši toplotni izolaciji. Nadalje so ugotavili, da se pri dani (izbrani) debelini materiala z zmanjšanjem števila odbojnikov primerno izboljšajo izolativne lastnosti materialov zdeli z nizko in srednjo gostoto. Optimiranje in kontrola gostote plasti v vsakem delu je prav tako pomembna za učinkovito delovanje večplastnih izolacijskih materialov s spreminjajočo se gostoto plasti. Predstavili so tudi teoretične vidike problemov izdelave večplastnih negorljivih materialov in uporabne reference za praktične inženirske aplikacije.

Ključne besede: upočasnjevanje ali zaviranje gorenja, večplastni izolacijski materiali, gostota plasti, proces šivanja, spreminjanje gostote

1 INTRODUCTION

Fossil fuels are the main energy resource worldwide.[1] However, in recent years, the need for air pollution control, environmental conservation and geopolitical security has shifted the attention to emerging cleaner energy sources such as hydrogen and natural gas. Effective storage is a key issue for these energy sources, with the liquid storage being preferable. Hydrogen and natural gas can be liquefied; in this form, they are referred to as liquid hydrogen (LH_2) and liquefied natural gas (LNG). Liquefaction has the advantages of high energy density and storage efficiency, convenient management and transportation. However, LH_2 and LNG require low-temperature storage as they have low boiling points and latent heats of vaporisation, and they evaporate readily.

*Corresponding author's e-mail:
chensp@lut.edu.cn (Shuping Chen)

Therefore, the containers used for storing LH_2 and LNG, called cryogenic liquid containers, must be thermally insulated to prevent heat loads[2–5].

The thermal insulation methods commonly employed for cryogenic liquid containers include bulk insulation, high-vacuum insulation, evacuated powder insulation, and multilayer insulation (MLI). MLI, also known as žsuperinsulation', is used most widely for cryogenic liquid containers owing to its outstanding insulation effect and typical apparent thermal conductivities of only 10^{-5}–10^{-6} W/(m·K) in a high-vacuum environment of 10^{-3} Pa. In addition, MLI is lightweight and environmentally friendly. As shown in Figure 1(a), cryogenic liquid containers generally have a double-wall structure consisting of an inner vessel, an outer vessel, and the vacuum-insulated annular space between the vessels. MLI materials, wrapped and mounted on the outer surface of the inner vessel as an insulation system, play an essential role in the vacuum-insulated annular space, directly contributing to the performance of cryogenic liquid containers.[6–8] As illustrated in **Figure 1b**, MLI materials are placed between the inner and outer vessels of a cryogenic storage tank and consist of reflector layers with low emissivities (grey vertical lines) and spacer layers with low thermal conductivities (dashed red lines). These inhibit thermal radiation (magenta arrows), gas conduction (blue arrows) and solid conduction (yellow arrows).

There is usually a temperature differential of hundreds of degrees Celsius between the cold mass of a cryogenic liquid and the surrounding environment, which results in a strong radiative heat transfer between the inner and outer vessels. The arrangement of reflectors can effectively reduce thermal radiation. Increasing the number of reflectors installed reduces thermal radiation to a greater extent. The layer density – the total number of reflector layers divided by the thickness of the MLI system – is related to the vacuum-pumping effect inside the MLI materials: the evacuation quality is reflected in the amount of the residual-gas conduction. Moreover, the layer density is also related to the magnitude of the thermal contact resistance and contact area among the layers of MLI materials. Thus, the layer density is an important factor to be considered in the design of an MLI system.[9] This study experimentally evaluates the influence of the layer density on the thermal insulation performance of MLIs. Johnson et al. reported that seam designs affect the insulation performance of MLI systems.[10] Therefore, this study tested the thermal performance of MLI using two seaming processes (**Figure 2**): the overlapped and the fold-over processes, with the same number of reflector layers and similar wrapping tightness. Variable-density multilayer insulation (VDMLI) is a key factor in enhancing insulation performance. In VDMLI, one layer of reflector and N layers of spacers (N > 1) constitute a composite layer of the cold-end segment, and a number of composite layers are configured to reduce the layer density by adjusting the number of spacers within a composite layer. In the hot-end segment, a layer of the reflector and a layer of the spacer are combined into a composite layer, and a corresponding number of composite layers are arranged. VDMLI is an advanced and notable technology in the field of multilayer insulation. It can specifically reduce solid conduction dominated by the cold-end segment, weaken the thermal radiation playing the major role in the hot-end segment, and decrease the total heat transfer.

The initial research conducted by NASA, comparing VDMLI with uniform-density multilayer insulation (UDMLI) showed that VDMLI provides superior thermal protection in cryogenic storage applications.[11,12] Hastings et al.[13] observed that VDMLI can attain the same insulation performance as UDMLI with less material. Zheng[14] found that, compared with a 50-reflector-layer UDMLI, the heat leakage of VDMLI with the same layer number was 13.53 % lower, and the heat flux was 17.49 % lower, proving that VDMLI exhibits better thermal insulation performance.

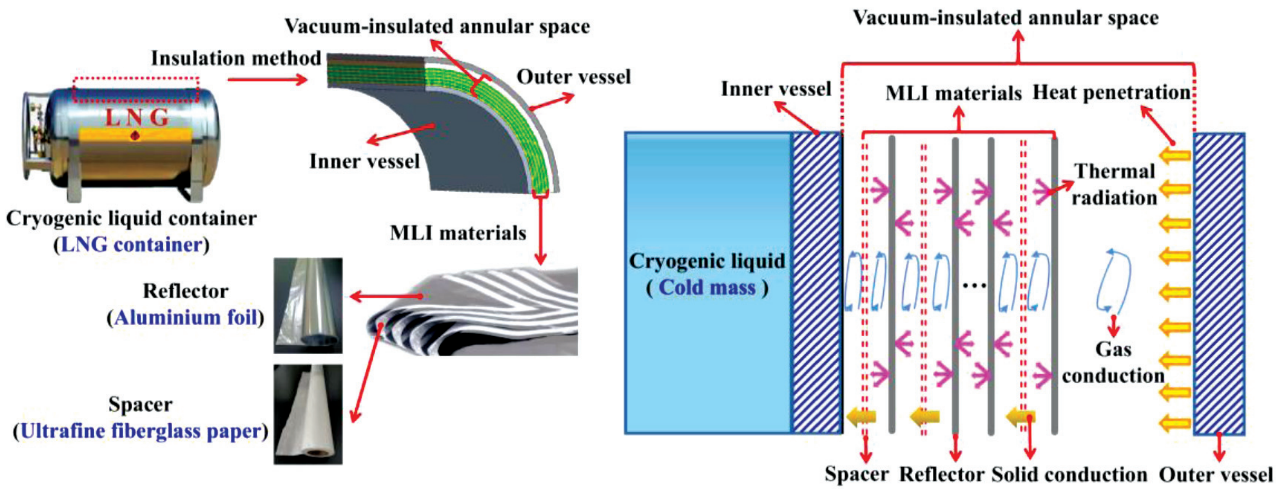

Figure 1: MLI material application and internal thermal-transfer mechanism

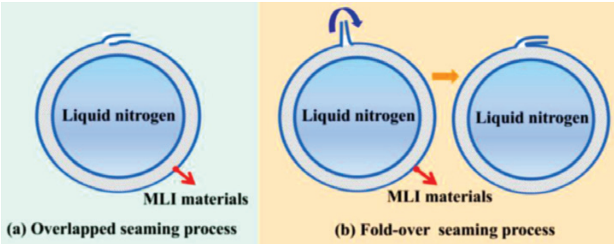

Figure 2: Two seaming processes used for wrapping MLI materials

The standards governing the construction of vehicular cryogenic LNG containers and application of MLI materials, such as GB/T 34510-2017 and ASTM C740/C740M-13, require that the cryogenic liquid containers intended for the storage of flammable and explosive energy sources like LH_2 or LNG are protected by flame-retardant insulation materials placed in the annular space.[15,16] Therefore, the thermal insulation performance of flame-retardant MLI materials must be tested and elucidated, and the factors affecting the insulation performance must be investigated.

Most theoretical and experimental studies on the insulation properties of MLI materials focussed on aerospace applications, and the selected research materials were mostly non-flame-retardant MLI materials with aluminised Mylar/Dacron net combinations; experimental studies on flame-retardant MLI materials are rare.[17–19] In this study, the thermal performance of flame-retardant MLI materials were experimentally investigated, considering the following aspects: layer density, seaming process, number of reflector layers and VDMLI arrangement. The findings and conclusions of this study may facilitate the design of MLI structures for applications in cryogenic liquid containers, which are especially suitable for cryogenic containers for storing flammable cryogenic liquids.

2 EXPERIMENTAL METHODS AND MATERIALS PREPARATION

2.1 Experimental method

Static liquid-nitrogen boil-off calorimetry is a standard method for testing the thermal-insulation performance of MLI materials, as shown in **Figure 3**. Its experimental platform can be divided into four subsystems: liquid-nitrogen filling, vacuum pumping, data acquisition, and calorimeter. The liquid-nitrogen-filling subsystem, responsible for introducing liquid nitrogen into the LN_2 boil-off calorimeter, comprises two self-pressurised cryogenic dewars, their corresponding pipes and several cryogenic valves. The vacuum-pumping unit consists of rotary-vane and turbo-molecular-vacuum pumps capable of evacuating the vacuum chamber to 10^{-5} Pa. The data-acquisition subsystem includes a digital vacummeter, gas-mass flowmeter, thermometers and auxiliary devices (such as a temperature-inspecting instrument and a data-acquisition computer) for monitoring the operation of the experimental set-up and collecting experimental data. The technical parameters of the key instruments of the data-acquisition subsystem are listed in **Table 1**.

Table 1: Technical parameters of the key instruments of the data-acquisition subsystem

Instruments	Digital vacuometer	Gas-mass flowmeter	Thermometer
Brand	EDWARDS	ALICAT	TPQE
Model	nWRG	SCIENTIFIC M-Series	PT100
Measurement range	10^{-7} to 10^{5} Pa	0 to 300 SCCM	70 to 720 K

In the calorimeter subsystem, the inner barrel of the LN_2 boil-off calorimeter consists of three cylindrical vessels: the upper-guard, test, and lower-guard cylinders, all

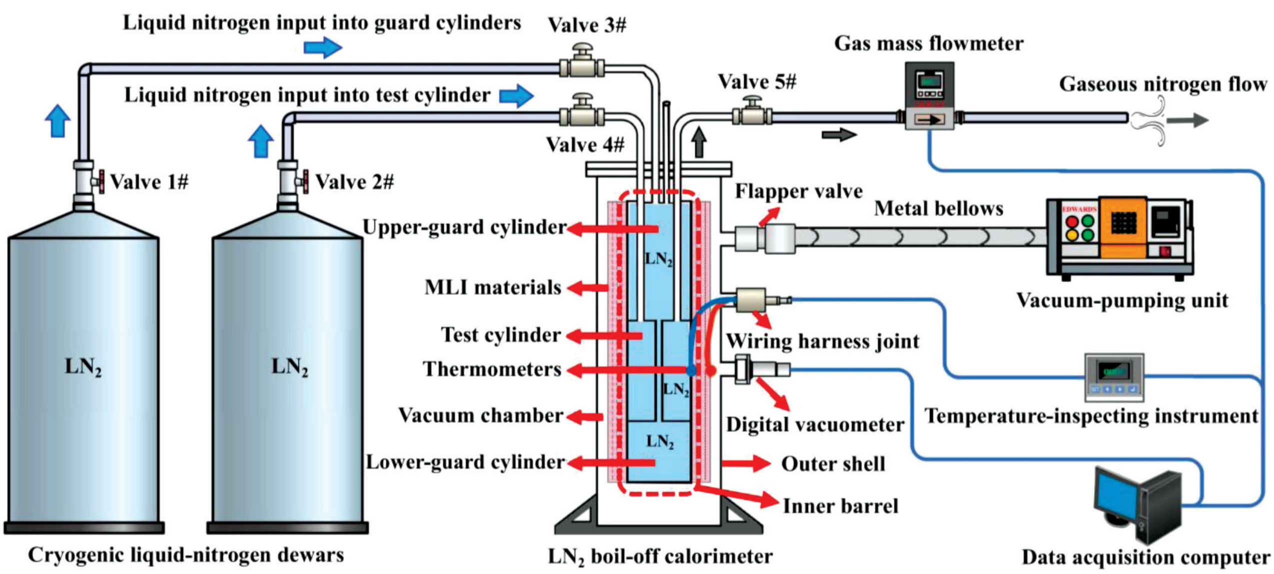

Figure 3: Schematic diagram of the standard static liquid-nitrogen boil-off calorimetry

of which are installed in the vacuum chamber (inside the outer shell). The flame-retardant MLI materials must be wrapped around the surface of the inner barrel for testing, as shown in **Figure 4a**.

In this study, the flame-retardant MLI materials were pre-treated based on the relevant standards such as GB/T 31480-2015. They were wound evenly on the inner barrel of the calorimeter using the clamshell approach: each MLI quilt, which contained 5 layers of reflectors and corresponding spacers, was wrapped individually around the inner barrel to be insulated.[20,21] The number of winding layers was recorded, and the wrapping thickness of the MLI structure was measured. Thermometers were arranged and fixed on the surfaces of the inner barrel and outermost reflector to record the cold and warm boundary temperatures of the MLI structure, respectively. Subsequently, the inner barrel was placed into the outer shell of the calorimeter using a crane to ensure that the surfaces of the MLI materials were not damaged during the insertion process.

After sealing the calorimeter, the vacuum-pumping unit was used. After the vacuum chamber was evacuated to less than 0.1 Pa, the guard and test cylinders were filled with liquid nitrogen. After the liquid-nitrogen filling, the pressure in the vacuum chamber, also known as cold vacuum pressure, smoothly decreased to an order of magnitude of 10^{-4} Pa and was always maintained below 1×10^{-3} Pa throughout the testing process. After the first filling operation, the calorimeter remained idle for 30 min while the evacuation system continued to run. After the inner barrel of the calorimeter and the MLI materials cooled down completely and the internal system approached thermal equilibrium, liquid nitrogen was re-added into the inner barrel to compensate for the evaporation loss, and then the system was ready for data acquisition.

In the data-recording stage, liquid nitrogen was filled into the guard cylinders of the calorimeter approximately every 10 min to ensure the presence of sufficient liquid nitrogen in the guard cylinders to fully block the heat leaking into the test cylinder of the calorimeter from the upper and lower longitudinal directions, ensuring the accuracy of the test data. **Figure 4b** illustrates the testing site of the insulation-performance analyses for the flame-retardant MLI materials.

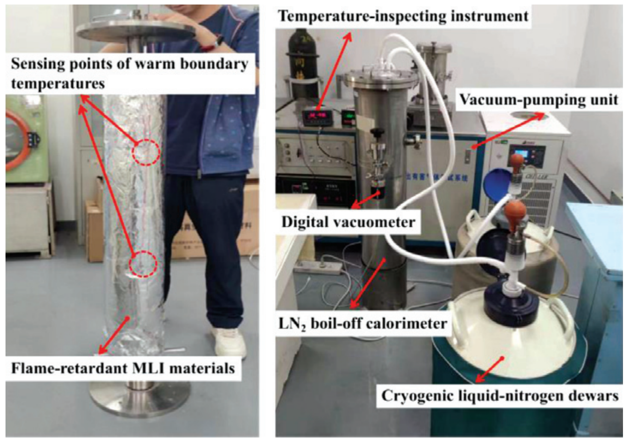

Figure 4: Wrapping material and the experimental set-up

The test data collected included the cold and warm boundary temperatures of the MLI structures and gaseous nitrogen flow rates passing through the gas mass flowmeter after the vaporisation and evaporation of liquid nitrogen. When the variation in the gas flow between any two time intervals was less than 5 %, the calorimeter system was considered to be stabilised, achieving thermal balance. The flowmeter values and boundary temperatures of the MLI materials were then recorded every 10 min for the next hour.

2.2 Materials preparation

For this study, the flame-retardant MLI materials, widely used on the Chinese mainland, were purchased from a related manufacturer. The properties of the materials are listed in **Table 2**.

To investigate the factors affecting the thermal performance, eight experimental groups were tested in this study, which included UDMLI and VDMLI arrangements. Layout schemes were also designed for the flame-retardant MLI materials. **Table 3** shows the de-

Table 2: Material properties

MLI	Material type	Properties
Reflector	Aluminium foil	Compatible with oxygen; Thickness of 0.0065 ± 6 % mm; Longitudinal tensile strength = 0.27 kN/m; Bright and continuous, consistent light transmittance, uniformity greater than ±5 %, no black spots.
Spacer	Cryogenic alkali-free ultrafine fibreglass paper	Compatible with oxygen; Thickness = 0.06 mm; Density of 12 ± 2.0 g/m^2; Longitudinal tensile strength = 0.04 kN/m; Moisture content = 0.5 %; Combustible matter content = 1 %; Thermal conductivity = 0.037 W/(m·K).

Table 3: Wrapping details of the flame-retardant MLI materials with the UDMLI arrangement

No. of serial experiments	Layer density *x* (layers/mm)	Number of reflectors	Number of spacers	Wrapping thickness (mm)	Types of seaming process
Exp. 1	4.47	60	60	13.4	Overlapped seaming process
Exp. 2	3.08	60	60	19.5	Overlapped seaming process
Exp. 3	2.50	60	60	24.0	Overlapped seaming process
Exp. 4	2.58	60	60	23.3	Fold-over seaming process
Exp. 5	2.98	70	70	23.5	Fold-over seaming process
Exp. 6	2.79	80	80	28.7	Fold-over seaming process

Table 4: Wrapping details of the flame-retardant MLI materials with the VDMLI arrangement

No. of serial experiments		Exp. 7	Exp. 8
Low-density segment	Number of reflectors	10	20
	Number of spacers	30	60
	Thickness of the segment (mm)	5.52	9.89
	Layer density x_L (layers/mm)	1.81	2.02
Medium-density segment	Number of reflectors	10	20
	Number of spacers	20	40
	Thickness of the segment (mm)	4.57	6.76
	Layer density x_M (layers/mm)	2.19	2.96
High-density segment	Number of reflectors	40	20
	Number of spacers	40	20
	Thickness of the segment (mm)	11.14	4.84
	Layer density x_H (layers/mm)	3.59	4.13
Total number of layers of reflectors		60	60
defaultTotal number of layers of spacers		90	21.49120
Wrapping thickness of VDMLI (mm)		21.23	
Seaming process		Overlapped seaming process	

tailed layout parameters of the UDMLI arrangements, and the details of the VDMLI arrangements are presented in **Table 4**. The differences between UDMLI and VDMLI are illustrated in **Figure 5**. UDMLI refers to the alternating arrangement of one layer of the reflector and one layer of the spacer from the cold boundary to the warm boundary of the insulation structure. The VDMLIs in this study were divided into three density segments: low-, medium- and high-density segments, with spacer-reflector ratios of 3:1, 2:1 and 1:1, respectively. The measurement experiments were performed using the standard static liquid-nitrogen boil-off calorimetry.

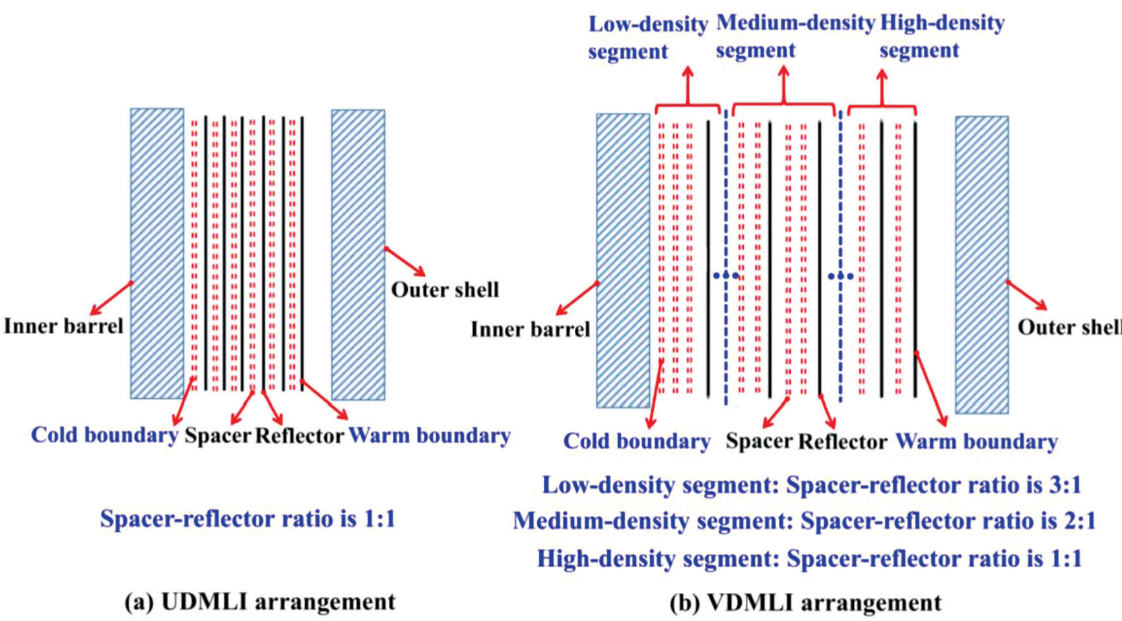

Figure 5: Schematic illustration of the differences between UDMLI and VDMLI arrangements

3 MEASUREMENT UNCERTAINTIES

The heat-leakage values of the flame-retardant MLI structures involved in the experiments were obtained using Equation (1), and the results for the eight experimental groups have been collated in **Table 5**. Heat leakage can be considered a one-dimensional thermal transfer from outside to inside, along the radial direction of the calorimeter in the normal direction of the material surface.

The heat leakage of MLI materials is given by:[22]

$$Q = VL\rho_g\left(\frac{T_0}{T_1}\right)\left(\frac{P_1}{P_0}\right) \tag{1}$$

where Q is the heat leakage through the MLI, W; V is the boil-off gas flow rate collected by the flowmeter, m^3/s; L represents the latent heat of the vaporisation of liquid nitrogen, J/kg; ρ_g is the density of gaseous nitrogen at 273.15 K, kg/m^3; P_1 and T_1 are the pressure and temperature at the outlet of the flowmeter, Pa and K, respectively; P_0 is the standard atmospheric pressure of 1.01325×10^5 Pa; T_0 is the thermodynamic temperature in the standard state, which is 273.15 K.

Researchers and engineers usually use heat flux and apparent thermal conductivity to characterise the thermal insulation effects of MLI materials. The heat flux refers to the heat leakage through the unit area of insulation materials in the normal direction of the material surface under a steady-state heat-transfer process. The apparent thermal conductivity refers to the heat leakage through a unit of insulation material per time unit under the steady-state heat-transfer process with known cold and warm boundary temperatures.

According to one-dimensional steady-state thermal conduction theory, the heat flux and apparent thermal conductivity of MLI materials can be expressed as follows[23]:

$$q = \frac{Q\cdot\ln(D_0/D_i)}{\pi l(D_0 - D_i)} \tag{2}$$

$$\lambda = \frac{Q\cdot\ln(D_0/D_i)}{2\pi l\cdot\Delta T} \tag{3}$$

where q is the heat flux, W/m^2; D_0 is the outer diameter of the wrapped MLI structures, m; D_i is the inner diameter of the wrapped MLI structures, m; l represents the length of the test cylinder of the calorimeter inner barrel, m; λ represents the apparent thermal conductivity, W/(m·K); and ΔT is the temperature difference between the warm and cold boundaries of the wrapped MLI structures, K.

By comparing the heat fluxes and apparent thermal conductivities, this study analyses and determines the effects of layer density, seaming process, number of reflector layers and VDMLI arrangement on the insulation performance of flame-retardant MLI materials.

In addition, measurement uncertainties are related to testing accuracy and are important for the credibility of experimental results. A summary of the measurement uncertainties of the LN_2 boil-off calorimeter is presented in **Table 6**. Uncertainties Q, q and λ can be obtained as follows:[5,24]

$$\frac{u_Q}{Q} = \sqrt{\left(\frac{\partial \ln Q}{\partial V}\right)^2 u_V^2} \tag{4}$$

$$\frac{u_q}{q} = \sqrt{\left(\frac{\partial \ln q}{\partial Q}\right)^2 u_Q^2 + \left(\frac{\partial \ln q}{\partial D_0}\right)^2 u_{D_0}^2 + \left(\frac{\partial \ln q}{\partial D_i}\right)^2 u_{D_i}^2 + \left(\frac{\partial \ln q}{\partial l}\right)^2 u_l^2} \tag{5}$$

$$\frac{u_\lambda}{\lambda} = \sqrt{\left(\frac{\partial \ln \lambda}{\partial Q}\right)^2 u_Q^2 + \left(\frac{\partial \ln \lambda}{\partial (D_0/D_i)}\right)^2 u_{(D_0/D_i)}^2 + \left(\frac{\partial \ln \lambda}{\partial l}\right)^2 u_l^2 + \left(\frac{\partial \ln \lambda}{\partial \Delta T}\right)^2 u_{\Delta T}^2} \tag{6}$$

Based on Equations (4)-(6) and **Table 6**, uncertainties Q, q and λ were estimated to be 1.72 %, 1.74 %, and 1.96 %, respectively.

4 RESULTS AND DISCUSSION

4.1 Layer density

The performance of flame-retardant MLI materials depends on the design and arrangement of the layer density. Theoretically, a lower layer density is conducive to less heat flux and higher insulation efficiency. This is caused by a reduction in the layer-to-layer contact area, an increase in the contact thermal resistance, and improvement of vacuum conditions. Using Equations (1)-(3), the heat fluxes and apparent thermal conductivi-

Table 5: Heat leakage measured for exps. 1 to 8

Serial experiments	Exp. 1	Exp. 2	Exp. 3	Exp. 4	Exp. 5	Exp. 6	Exp. 7	Exp. 8
Heat leakage Q (W)	0.390	0.311	0.205	0.153	0.150	0.136	0.208	0.323

Table 6: Measurement uncertainties of the LN_2 boil-off calorimeter

Symbols	Description	Units	Uncertainties
V	Boil-off gas flow rate	m^3/s	± (0.8 % of reading + 0.2 % of full scale)
D_o D_i l	Outer/inner diameter Length of the test cylinder	m	± 0.2 % of reading
ΔT	Temperature difference	K	± 0.5 % of reading

ties of Exps. 1, 2 and 3 were obtained, as shown in **Figure 6**, reflecting the influence of layer density on the insulation performance.

As mentioned above in **Table 3**, Exps. 1, 2 and 3 have the same number of reflectors – 60 layers of aluminium foil – and the overlapped seaming process is adopted uniformly at the material junction; they differ only in the layer density. The layer density in Exp. 1 is 4.47 layers/mm, while those of Exps. 2 and 3 are 3.08 and 2.50 layers/mm, respectively. When the MLI materials are wrapped more loosely, the lower layer densities result in thicker MLI structures and better thermal insulation effects. Of these groups, Exp. 3 demonstrated the best thermal insulation performance, with a minimum heat flux of 1.151 W/m^2 and the smallest apparent thermal conductivity of 1.319 × 10^{-4} W/(m·K). A comparison of Exps. 1 and 2 indicates that the layer density in Exp. 2 is 31.10 % lower than that observed in Exp. 1, while the heat flux is 23.25 % lower. The layer density and heat flux of Exp. 3 are 18.83 % and 35.77 % lower than those of Exp. 2, respectively. These results indicate that a layer density in a range of 2.5–3.0 layers/mm can effectively diminish the heat flux and improve the thermal insulation performance. The apparent thermal conductivities of the three experimental groups were similar, and the maximum fluctuation range was approximately 20 %, which is typical. Thus, reducing the layer density can significantly reduce the heat flux; this observation may be useful for engineering practice.

4.2 Seaming process

As illustrated in **Figure 7**, both Exps. 3 and 4 used 60 layers of aluminium foil as reflectors, and their layer densities were similar, 2.50 layers/mm and 2.58 layers/mm, respectively. However, the groups differed in the seaming technique employed during the material wrapping process. Exp. 3 adopted an overlapped seaming process, whereas Exp. 4 adopted a fold-over seaming process. Exp. 4, using the fold-over seaming process, demonstrated a better insulation performance, with less heat flux and a smaller apparent thermal conductivity than that of Exp. 3. The heat flux of Exp. 4 was 0.863 W/m^2, which was 25.02 % lower than that of Exp. 3. The apparent thermal conductivity of Exp. 4 was 9.248 × 10^{-5} W/(m·K), which was 29.89 % lower than that of Exp. 3. Thus, the fold-over seaming used at the joints of materials is better for enhancing the insulation performance of flame-retardant MLI structures than the overlapping process.

4.3 Layer number of reflectors

As observed in **Figure 8**, the MLI structures in Exps. 4, 5 and 6 exhibited a good thermal insulation performance, with heat fluxes of less than 1 W/m^2. Given that the layer densities were in the 2.5–3.0 layers/mm range and the seaming process remained the same, the performance of the MLI structures was effectively improved with an increase in the number of reflector layers. In Exp. 6, the heat flux of the MLI structure with 80 reflectors was 0.742 W/m^2, which was 14.02 % and 12.19 % less than for Exps. 4 and 5, respectively. This is because an increase in the number of reflectors can further weaken the radiative heat transfer, thus reducing the total environmental heat infiltration. In contrast, a larger number of reflective layers result in thicker MLI structures, necessitating a more complex installation, a greater outgassing amount (which reduces the vacuum life of the cryogenic liquid containers) and a costlier insulation system.[25,26] Therefore, the layer number of reflectors used needs to be matched to the requirements of the actual application.

The apparent thermal conductivities of these three experiments were successfully reduced to the order of 10^{-5} W/(m·K). In addition, the decrease in the heat flux between Exps. 6 and 5 was significantly greater than that between Exps. 5 and 4. The reason for it may be that the layer density of Exp. 5 was 2.98 layers/mm, which is slightly higher than those of Exps. 4 and 6, which may have negatively affected the insulation performance. The

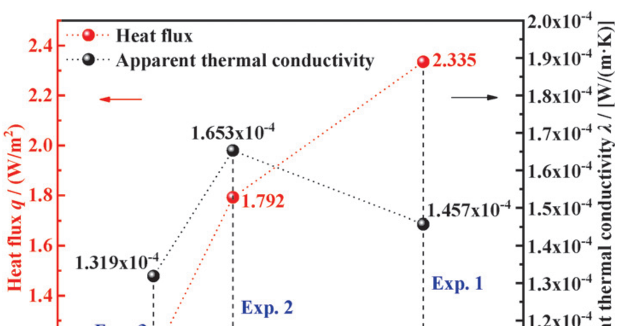

Figure 6: Comparison of the heat fluxes and apparent thermal conductivities of Exps. 1, 2, and 3

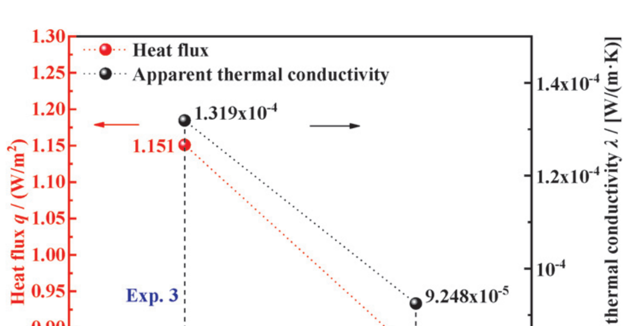

Figure 7: Comparison of heat fluxes and apparent thermal conductivities between Exps. 3 and 4

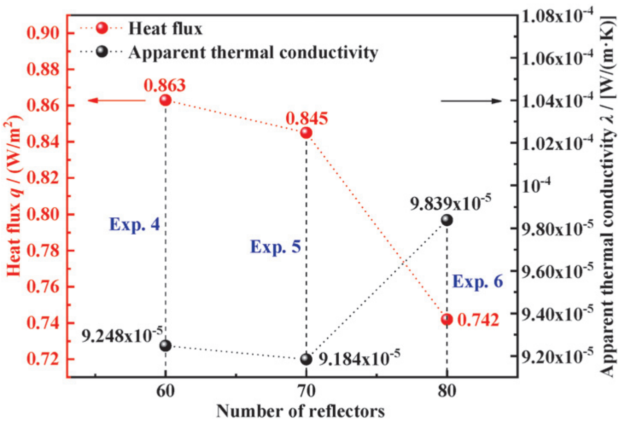

Figure 8: Comparison of the heat fluxes and apparent thermal conductivities of Exps. 4, 5 and 6

thermal insulation performance of UDMLI results from multiple combined factors such as layer density, seaming process, and the number of reflectors. Therefore, further reducing the layer density of Exp. 5 may result in a smaller heat flux.

4.4 VDMLI arrangement

As shown in **Figure 9**, two types of VDMLI are considered in this study: Exps. 7 and 8. However, the numbers of composite layers (the numbers of reflectors) allocated to the low-, medium- and high-density segments are different. The layout schemes of the VDMLI in Exps. 7 and 8 are described in detail in **Table 4**. The wrapping thicknesses of Exps. 7 and 8 were similar, but the number of spacers in Exp. 7 was 25 % lower than that in Exp. 8. As demonstrated in **Figure 9**, the insulation performance of Exp. 7 was better than that of Exp. 8. The heat flux of Exp. 7 was 35.42 % lower than that of Exp. 8, and the apparent thermal conductivity was 37.98 % lower, with values of 1.187 W/m^2 and 1.158 × 10^{-4} W/(m·K), respectively. This shows that, under the condition of a certain wrapping thickness of the VDMLI structure, an appropriate reduction of the number of reflectors in the low- and medium-density segments and a decrease in their thicknesses can not only reduce the material usage and save the cost but also contribute to improving the insulation performance.

Exps. 2 and 7 inckuded UDMLI and VDMLI with the same number of 60 reflector layers, and the wrapping thicknesses were similar, 19.48 mm and 21.23 mm, respectively. The heat flux of Exp. 7 was 33.76 % lower than that of Exp. 2, and the apparent thermal conductivity was 29.95 % lower therein. Thus, given the same number of reflector layers and a similar wrapping thickness, the VDMLI arrangement exhibits a better thermal insulation performance than the UDMLI arrangement.

Notably, the results of Exps. 3 and 7 were relatively close, with the same number of reflector layers but different thicknesses. Theoretically, the performance of VDMLI in Exp. 7 was expected be better than that of UDMLI in Exp. 3. Analysis showed the layer density to be the cause of the observed phenomenon. The layer density of Exp. 3 was 2.50 layers/mm, which is appropriate and suitable. The layer density of each density segment in Exp. 7 was excessive, and even the layer density of the high-density segment was greater than 3.5 layers/mm. This observation also explains why Exp. 8 exhibited an insulation performance inferior to Exps. 2 and 3. When the high-density segment of Exp. 8 was compared with the densities of Exps. 2 and 3, the layer density of the high-density segment was 4.13 layers/mm, which was 1.34 times that of Exp. 2 and 1.65 times that of Exp. 3. These phenomena further indicate that the insulation performance of flame-retardant MLI materials is the result of a combination of various factors such as the number of reflectors, layer density and UDMLI or VDMLI arrangements. For VDMLI, the handling and control of layer densities of each density segment must be addressed. The various influential factors must be comprehensively optimised to enhance the thermal insulation effect.

Table 7 summarises the results of the thermal-insulation-performance tests of the flame-retardant MLI materials obtained with Exps. 1 to 8, sharing the data and providing a reference for the thermal insulation design of cryogenic liquid containers storing flammable and explosive energy sources like LH_2 or LNG.

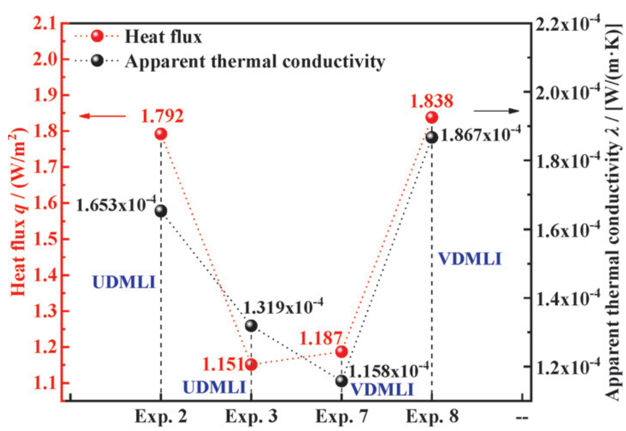

Figure 9: Comparison of the heat fluxes and apparent thermal conductivities from Exps. 2, 3, 7 and 8

Table 7: Thermal-insulation-performance indexes obtained with Exps. 1 to 8

Serial Experiments	Heat leakage Q	Heat flux q	Apparent thermal conductivity λ
	(W)	(W/m^2)	(W/(m·K))
Exp. 1	0.390	2.335	1.457 × 10^{-4}
Exp. 2	0.311	1.792	1.653 × 10^{-4}
Exp. 3	0.205	1.151	1.319 × 10^{-4}
Exp. 4	0.153	0.863	9.248 × 10^{-5}
Exp. 5	0.150	0.845	9.184 × 10^{-5}
Exp. 6	0.136	0.742	9.839 × 10^{-5}
Exp. 7	0.208	1.187	1.158 × 10^{-4}
Exp. 8	0.323	1.838	1.867 × 10^{-4}

5 CONCLUSIONS

In this study, the thermal insulation properties of eight groups of flame-retardant MLI materials were tested, and the effects of four factors – layer density, seaming process, number of reflector layers and VDMLI arrangement – on the insulation performance of MLI structures were analysed. As a result, the following conclusions are drawn:

A moderate reduction in the wrapping tightness of flame-retardant MLI structures, i.e., a decrease in their layer densities, can effectively reduce the heat leakage and flux and improve the insulation performance. In this study, when the layer density was reduced by 44.07 %, the heat leakage and heat flux were reduced by 47.44 % and 50.71 %, respectively. In the 2.5–3.0 layers/mm range, the heat flux decreased significantly with the layer density. However, in practical engineering applications, the size of the vacuum-insulated annular space of a cryogenic liquid container must also be considered. Therefore, the layer density of materials should be appropriately decreased within a limited space.

The fold-over seaming process better enhances the thermal insulation performance of flame-retardant MLI materials than the overlapped seaming process. The fold-over seaming process leads to less heat leakage and heat flux, and better apparent thermal conductivity. As a result, the choice of the seaming process plays a significant role in improving the insulation performance of flame-retardant MLI structures.

Adding more reflector layers can reduce the radiative heat transfer and further decrease the heat leakage and flux. In this study, when the number of reflector layers was increased by 33.33 %, the heat leakage decreased by 11.11 % and the heat flux was reduced by 14.02 %. In engineering practice, the number of reflectors can be determined by the type of cryogenic liquid stored. For cryogenic LH_2 containers, the number of reflectors in the MLI system ranges from 80 to 120 layers. For cryogenic LNG containers, this number ranges from 40 to 60 layers. When the number of reflectors is fixed, the MLI system can achieve an outstanding insulation performance with an appropriate layer density and proper wrapping technique. However, a higher number of reflectors can result in increased production cost and increased material outgassing volume.

For the 60-layer-reflector VDMLI arrangement, the number of reflectors in low- and medium-density segments is suggested to be limited to 10 layers or fewer, and the layer density should be paid attention to and carefully controlled in each density area.

The minimum heat flux was achieved in Exp. 6 (0.742 W/m^2). The minimum apparent thermal conductivity was obtained in Exp. 5 (9.184×10^{-5} W/(m·K)). The data and wrapping parameters for flame-retardant MLI materials can help improve the insulation design for cryogenic LH_2 or LNG containers and provide meaningful reference values for practical engineering applications.

Acknowledgement

This study was financially supported by the Natural Science Foundation of the Gansu Province, China (21JR7RA269).

Nomenclature

D_o: Outer diameter of MLI (m)
D_i: Inner diameter of MLI (m)
l: Length of the test cylinder of the calorimeter inner barrel (m)
L: Latent heat of the vaporisation of liquid nitrogen (J/kg)
P_0: Standard atmospheric pressure (Pa)
P_1: Pressure at the outlet of the flowmeter (Pa)
q: Heat flux through MLI (W/m^2)
Q: Heat leakage through MLI (W)
T_0: Standard thermodynamic temperature (K)
T_1: Temperature at the outlet of the flowmeter (K)
V: Boil-off gas flow rate (m^3/s)
x: Layer density of UDMLI arrangements (layers/mm)
x_L: Layer density of the low-density segment in VDMLI (layers/mm)
x_M: Layer density of the medium-density segment in VDMLI (layers/mm)
x_H: Layer density of the high-density segment in VDMLI (layers/mm)
ΔT: Temperature difference between warm and cold boundaries of MLI (K)
λ: Apparent thermal conductivity of MLI (W/(m·K))
ρ_g: Density of gaseous nitrogen at 273.15 K (kg/m³)

6 REFERENCES

[1] BP Statistical Review of World Energy 2022, https://www.bp.com/content/dam/bp/business-sites/en/global/corporate/pdfs/energy-economics/statistical-review/bp-stats-review-2022-full-report.pdf
[2] S. A. Sherif, N. Zeytinoglu, T. N. Veziroglu, Liquid hydrogen: Potential, problems, and a proposed research program, Int. J. Hydrogen Energy, 22 (**1997**) 7, 683–688, doi:10.1016/s0360-3199(96)00201-7
[3] M. Aziz, Liquid hydrogen: A review on liquefaction, storage, transportation, and safety, Energies, 14 (**2021**) 18, 1–29, doi:10.3390/en14185917
[4] C. Winnefeld, T. Kadyk, B. Bensmann, U. Krewer, R. Hanke-Rauschenbach, Modelling and designing cryogenic hydrogen tanks for future aircraft applications, Energies, 11 (**2018**) 1, doi:10.3390/en11010105
[5] B. Wang, R. Luo, H. Chen, C. Zheng, Y. Gao, H. Wang, A. R. Hashmi, Q. Zhao, Z. Gan, Characterization and monitoring of vacuum pressure of tank containers with multilayer insulation for cryogenic clean fuels storage and transportation, Appl. Therm. Eng., 187 (**2021**), doi:10.1016/j.applthermaleng.2021.116569
[6] P. M. Sutheesh, A. Chollackal, Thermal performance of multilayer insulation: A review, IOP Conf. Series: Materials Science and Engineering, Kerala State 2018, doi:10.1088/1757-899X/396/1/012061

[7] D. Singh, A. Pandey, M. K. Singh, L. Singh, V. Singh, Heat radiation reduction in cryostats with multilayer insulation technique, J. Instrum., 15 (**2020**), doi:10.1088/1748-0221/15/07/P07032

[8] X. Xu, H. Xu, B. Yang, L. Chen, J. Wang, A novel composite insulation system of hollow glass microspheres and multilayer insulation with self-evaporating vapor cooled shield for liquid hydrogen storage, Energy Technol., 8 (**2020**) 9, doi:10.1002/ente.202000591

[9] J. Demko, J. E. Fesmire, Q. Shu, Cryogenic Heat Management: Technology and Applications for Science and Industry, 1st ed., CRC Press, Boca Raton 2022, 69

[10] W. L. Johnson, J. E. Fesmire, Cryogenic testing of different seam concepts for multilayer insulation systems, Advances in Cryogenic Engineering: Transactions of the Cryogenic Engineering Conference – CEC, 2010, 905–912, doi:10.1063/1.3422447

[11] A. Hedayat, T. M. Brown, L. J. Hastings, J. Martin, Variable density multilayer insulation for cryogenic storage, 36th AIAA/ASME/SAE/ASEE Joint Propulsion Conference & Exhibition, Huntsville 2000, doi:10.2514/6.2000-3790

[12] J. J. Martin, L. Hastings, Large-scale liquid hydrogen testing of a variable density multilayer insulation with a foam substrate, NASA/TM-2001-211089, 2001

[13] L. J. Hastings, A. Hedayat, T. M. Brown, Analytical modeling and test correlation of variable density multilayer insulation for cryogenic storage, NASA TM-2004-213175, 2004

[14] J. Zheng, L. Chen, C. Cui, J. Guo, W. Zhu, Y. Zhou, J. Wang, Experimental study on composite insulation system of spray on foam insulation and variable density multilayer insulation, Appl. Therm. Eng., 130 (**2018**), 161–168, doi:10.1016/j.applthermaleng.2017.11.050

[15] GB/T 34510-2017 – Liquefied natural gas cylinders for vehicles, Standards Press of China, Beijing (in simplified Chinese)

[16] ASTM C740/C740M-13 – Standard guide for evacuated reflective insulation. In: Cryogenic Service, ASTM International, West Conshohocken, Pennsylvania

[17] Y. H. Huang, B. Wang, S. H. Zhou, J. Y. Wu, G. Lei, P. Li, P. J. Sun, Modeling and experimental study on combination of foam and variable density multilayer insulation for cryogen storage, Energy, 123 (**2017**), 487–498, doi:10.1016/j.energy.2017.01.147

[18] Z. Liu, Y. Li, F. Xie, K. Zhou, Thermal performance of foam/MLI for cryogenic liquid hydrogen tank during the ascent and on orbit period, Appl. Therm. Eng., 98 (**2016**), 430–439, doi:10.1016/j.applthermaleng.2015.12.084

[19] J. Zheng, L. Chen, J. Wang, X. Xi, H. Zhu, Y. Zhou, J. Wang, Thermodynamic analysis and comparison of four insulation schemes for liquid hydrogen storage tank, Energ. Convers. Manage., 186 (**2019**), 526–534, doi:10.1016/j.enconman.2019.02.073

[20] GB/T 31480-2015 – Materials for high vacuum multilayer insulation of cryogenic vessel, Standards Press of China, Beijing (in simplified Chinese)

[21] S. A. Dye, A. B. Kopelove, G. L. Mills, Wrapped multilayer insulation for cryogenic piping, Advances in Cryogenic Engineering: Transactions of the Cryogenic Engineering Conference – CEC, 2012, 1293–1298, doi:10.1063/1.4707053

[22] X. Shen, Study on an insulation performance testing system for high vacuum MLI, Master's Thesis, Zhejiang University, Hangzhou, China, 2013

[23] J. E. Fesmire, Standardization in cryogenic insulation systems testing and performance data, Phys. Procedia, 67 (**2015**), 1089–1097, doi:10.1016/j.phpro.2015.06.205

[24] J. H. Kim, T. W. Simon, R. Viskanta, Journal of heat transfer policy on reporting uncertainties in experimental measurements and results, J. Heat Transfer, 115 (**2018**) 1, 5–6, doi:10.1115/1.2910670

[25] Y. G. Shi, Research on outgassing characteristics of cryogenics insulation materials under vacuum condition, Master's Thesis, Lanzhou University of Technology, Lanzhou, China, 2022, doi:10.27206/d.cnki.ggsgu.2022.000462

[26] C. Zheng, Research on vacuum outgassing characteristics and testing methods of key materials of an LNG tank container, Master's Thesis, China Jiliang University, Hangzhou, China, 2021, doi:10.27819/d.cnki.gzgjl.2021.000360